Preparation, Characterization, and Mechanical Properties of Some Microcellular Polysulfone Foams

Hongliu Sun, James E. Mark

Department of Chemistry and the Polymer Research Center, The University of Cincinnati, Cincinnati, Ohio 45221-0172

Received 4 October 2001; accepted 18 January 2002

ABSTRACT: Several polymers were evaluated as candidates for the production of high-performance microcellular closed-cell foams. The polymers involved were a polysulfone, a polyethersulfone, a polyphenylsulfone, a polyetherimide, and a poly(ether ketone ketone), and their suitability was gauged by measuring rates at which they could be impregnated with carbon dioxide under pressure at room temperature. This step is essential to the subsequent step of heating the impregnated samples at various temperatures to create foamed structures. The present study focused primarily on the use of the polysulfone in this regard. Microcellular foams of this polymer were found to have average cell sizes in the range 1–10 μm and cell densities on the order of 10^{10}–10^{14} cells/cm^3. The microstructures of these foamed samples were controlled through careful choices of the foaming temperature and the foaming speed to produce a wide range of foam densities. Since these materials were prepared for possible use as structural materials, tensile tests were conducted to investigate the dependence of some of their mechanical properties on the foam densities (relative to those of the unfoamed polymer). The results indicated that the tensile moduli of these polysulfone foams increased with the square of their relative densities, and the tensile strengths were proportional to these densities. Both of these experimental findings are in agreement with theory. © 2002 Wiley Periodicals, Inc. J Appl Polym Sci 86: 1692–1701, 2002

Key words: poly(ether sulfone); high performance polymers; mechanical properties

INTRODUCTION

"Microcellular foams" are defined as having average cell sizes in the range 1–10 μm and cell densities on the order of 10^9–10^{15} cells/cm^3. Cells with such structures were proposed by Suh et al.[1,2] in the early 1980s as a means to reduce materials consumption and to increase the toughness of such cellular materials. The hypothesis of their work was that if the cell size was smaller than were the critical flaws preexisting in the polymer then material costs could be reduced without significantly compromising the mechanical properties. Their microcellular foaming process was performed in a two-stage batch approach.[3,4] In the first stage, the polymer sample was saturated at high pressure and at room temperature with a nonreactive gas (such as carbon dioxide or nitrogen). In the second stage, the pressure was released and the sample was then quickly heated to a temperature high enough to soften the polymer. The resulting thermodynamic instability in the gas-saturated polymer nucleated a myriad of bubbles or cells and resulted in foams with cell sizes the order of micrometers.

Most of the early work on such foams was restricted to predominantly amorphous polymers, such as polystyrene,[5–7] polypropylene,[8] poly(vinyl chloride),[9,10] and polycarbonate.[11–13] Recently, this technology has been extended to semicrystalline polymers, such as poly(ethylene terephthalate),[4,14,15] some liquid crystalline polymers, and some thermosets.[16,17] Some of these microcellular foams had advantages over conventional foams and their unfoamed counterparts. For example,[11] these foams typically exhibit high bend/shear strength, high rigidity, good impact strength, considerable toughness, large stiffness-to-weight ratio, and low thermal conductivity. With such unique properties, microcellular plastics gained a number of innovative applications in many fields, such as in packing materials, insulations, filtration membranes, sports equipment, and automobile and aircraft parts.

Currently, military aircraft use large amounts of cellular sandwich materials because of their superior stiffnesses and strengths (relative to the unfoamed starting materials). Most of the commercially available polymeric sandwich cores, however, have temperature capabilities to only 350°F. Alleviating this limitation was one of the aims of the present work. More generally, the goals were the preparation, characterization, and evaluation of polymer-based foams of sufficient toughness and high-temperature stability to be used as structural materials in Air Force applications. In this series of studies, a variety of commer-

Correspondence to: J. E. Mark.

Contract grant sponsor: Air Force Office of Scientific Research; contract grant number: F49620-98-1-0319.

Journal of Applied Polymer Science, Vol. 86, 1692–1701 (2002)

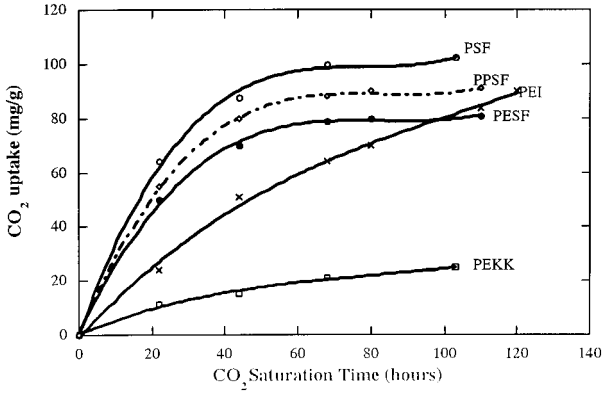

Figure 1 CO_2 sorption curves at 830 psi and room temperature.

cially available high-performance thermoplastics will be evaluated with regard to the extent to which they can be converted into monolithic foams for such applications.

There are three basic steps in the microcellular process[18–20]: gas/polymer solution formation, cell nucleation, and cell growth. The first step involves the absorption of an inert gas into the polymer matrix at high pressure to form a gas/polymer solution. Usually, there will be a high gas concentration in this solution (typically 3–20% by weight).[20] The solution formation is governed by gas diffusion into the polymer matrix. Since the diffusion process is typically very slow, this can lead to long cycle times, particularly in the case of thick samples. To produce microcellular foams at an acceptable industrial processing rate, improved techniques for rapid solution formation need to be developed. Once the gas/polymer

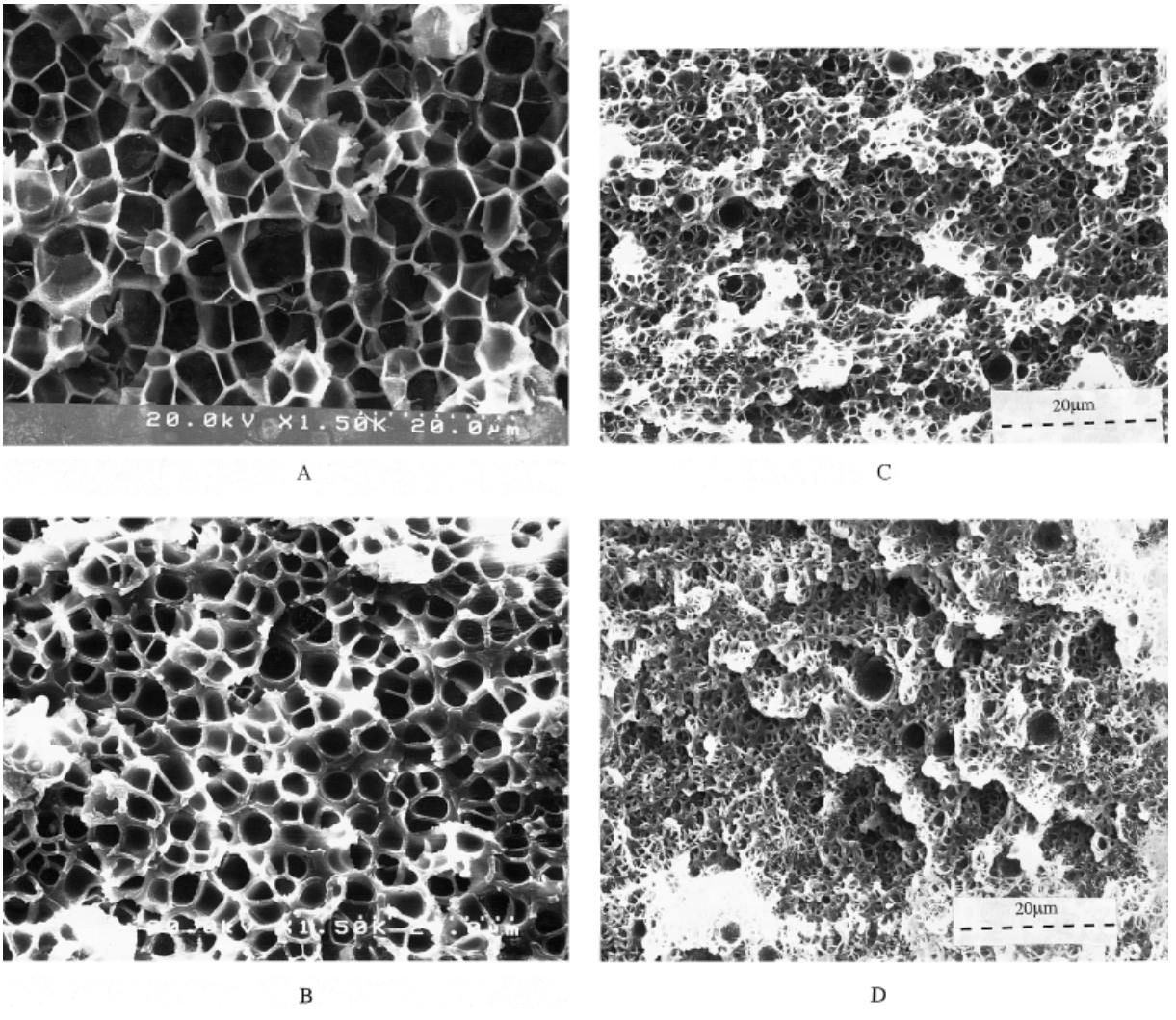

Figure 2 Typical SEM micrographs of microcellular foams: (A) PSF; (B) PESF; (C) PPSF; (D) PEI; (E) PEKK. Foaming conditions: saturation pressure: 830 psi; saturation time: 50 h for PSF, PESF, and PPSF and 120 h for PEI and PEKK: CO_2 contents: 9.3% for PSF; 9.0% for PPSF; PEI, 7.8 % for PESF; 2.6% for PEKK. For all polymers, the foaming temperature was 175°C and the foaming time was 30 s.

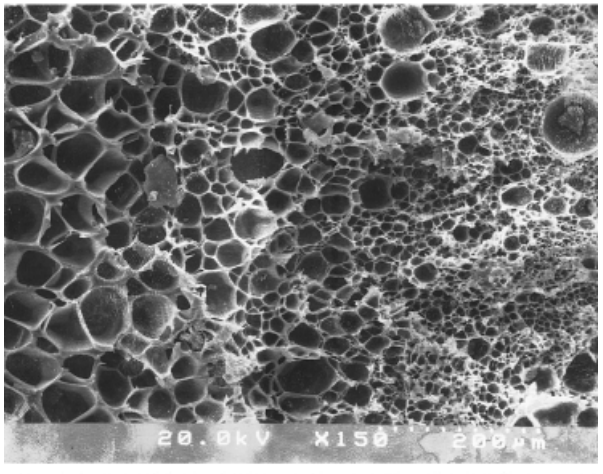

E

Figure 2 (*Continued from previous page*)

solution has formed, the next step is the rapid nucleation of very large numbers of bubbles in the solution by subjecting the gas/polymer solution to a large thermodynamic instability. This is accomplished by quickly changing the solubility of the gas in the solution by changing the temperature and pressure. The nucleation process is of crucial importance since it determines the cell morphology and the properties of the resulting foams. The final step is the growth of the stable nuclei. In this step, the gas molecules diffuse from the polymer matrix into the nucleated cell and allow cell growth to occur. This growth is controlled mainly by the foaming temperature, foaming time, and stiffness of the polymer chains.

Several polymers were evaluated as candidates for the production of such microcellular closed-cell foams. The polymers chosen were a polysulfone, a polyethersulfone, a polyphenylsulfone, a polyetherimide, and a poly(ether ketone ketone), and their suitability was gauged by measuring rates at which they could be impregnated with carbon dioxide under pressure at room temperature. The polysulfone was chosen for this first study, to illustrate the utility of the method. The structures of the foams from this polymer were controlled through the choice of foaming conditions to produce a wide range of foam densities. By carefully choosing the processing parameters, some structural aspects of the microcellular foam could be successfully controlled. The effects of the processing parameters (such as saturation time and pressure, foaming time, and temperature) on the relative densities and microcellular structures of these foams were documented. Since these materials were prepared for the possible use as structural materials, mechanical tests were also carried out to investigate the dependence of these properties on the relative foam densities.

EXPERIMENTAL

Materials

Polysulfone (PSF, Udel P-1700), polyethersulfone (PESF, Radel A-200), and polyphenylsulfone (PPSF, Radel R-5000) resins were kindly supplied by BP Amoco (Alpharetta, GA). The polymer resins were dried at 140°C about 8 h in an oven prior to melt processing. PSF and polyetherimide (PEI, Ultem 1000) polymer sheets (1.6 mm in thickness) were purchased from the Curbell Plastic Co. (Cincinnati, OH). Poly(ether ketone ketone) (PEKK) sheets (2.0 mm in thickness) were provided by DuPont (Belle, WV).

The glass transition temperatures, $T_{g's}$, and densities, $\rho_{m's}$, were as follows. PSF: 185°C and 1.24 g/cm^3; PESF: 220°C and 1.37 g/cm^3; and PPSF: 220°C and 1.29 g/cm^3. Carbon dioxide (99.9%) was obtained from Wright Brother's Inc. (Cincinnati, OH).

Preparation of polymer panels

PSF, PESF, and PPSF resins were compression-molded into panels (1.5 mm in thickness) with a hydraulic hot press (Carver Laboratory Press, Fred S. Carver Inc.) for 30 min using 3 tons of pressure. The temperature was either 250°C (for PSF) or 300°C (for PESF and PPSF). Rectangular strips were cut from the panel sheets and used for the foaming process.

Preparation of microcellular foams

Microcellular foaming experiments were performed in the now-standard two-stage batch process. In the first stage, the polymer samples were saturated in a pressure vessel with CO_2 gas maintained at a pressure of 830 psi and at room temperature (22–23°C). During the saturation, the samples were removed periodically from the pressure vessel and weighed on a precision balance with an accuracy of 10 μg. In all the foaming

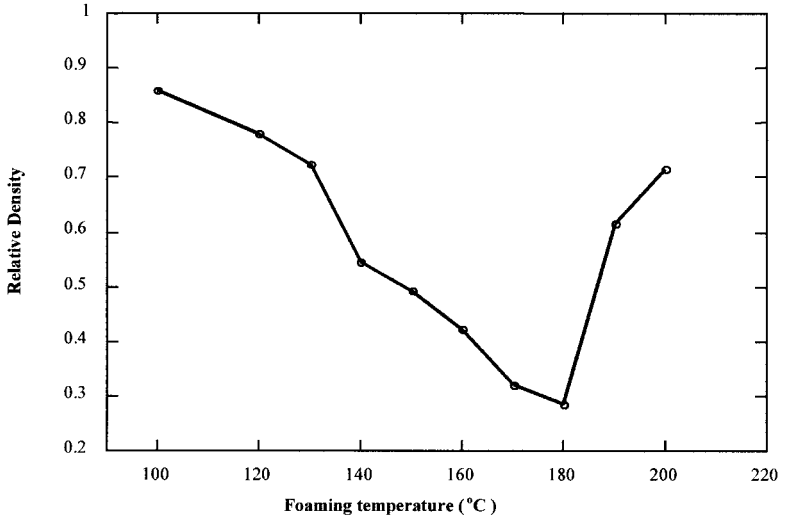

Figure 3 Relative densities of the PSF foams as a function of foaming temperature. The CO_2 content was 9% by weight and the foaming time was 30 s.

experiments, the saturation time for PSF, PESF, and PPSF was 50 h, and for PEI and PEKK, 120 h. The CO_2 gas concentration in the polymer samples was 9% for PSF, 8.5% for PPSF and PEI, 8% for PESF, and only 2.4% for PEKK. After the equilibrium amount of the gas had been absorbed, the pressure was quickly released, and the polymer samples were removed from the pressure vessel and weighed to determine the amount of gas absorbed. The samples were kept in air about 0.5 h before foaming, which gave the subsequently foamed samples a very smooth glossy surface. In the next stage, the supersaturated samples were foamed for a predetermined period of time in an oil bath maintained at the desired temperature. After foaming, the samples were quenched in cold water. This sudden quench locked in the microstructures of the resulting foams. After foaming, the original transparent polymer sheets became opaque and white and had smooth surfaces as integral skins.

Measurements of foam density

The foam density ρ_f was measured by water-displacement methods. Densities were calculated by measuring the volume of water displaced by the sample and dividing this volume into the sample mass. Because of the integral skin and closed-cell structure of the foam samples, there was no obvious uptake of water by the samples during the measurements. The relative foam density is the ratio of the density of the foam to the density of the unfoamed polymer.

SEM analyses

For scanning electron microscopy, the foamed samples were frozen in liquid nitrogen and fractured to ensure that the microstructure remained clean and intact. The fractured surfaces were coated with gold using a sputter coater and photographed with a scanning electron microscope (SEM, Hitachi S-4000).

Determinations of cell sizes and cell densities

The resulting SEM micrographs were analyzed by Pro-Plus Image Analysis Software to measure cell sizes and size distributions. Usually, SEM micrographs containing 100–200 cells were used in the image analysis.

The cell density N_0 is the number of cells nucleated per unit volume (cm^3) of the original unfoamed polymer. It was calculated from the SEM micrographs using the method suggested by Kumar and Weller[21]:

$$N_0 = [nM^2/A]^{3/2}[1/(1 - V_f)] \quad (1)$$

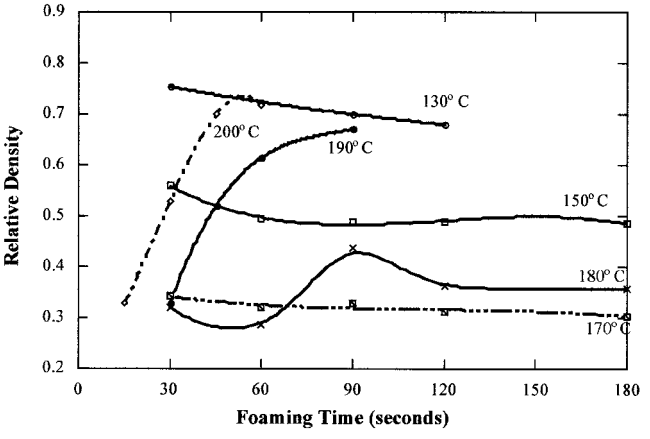

Figure 4 Relative densities of the foams as a function of foaming time (9% CO_2 by weight).

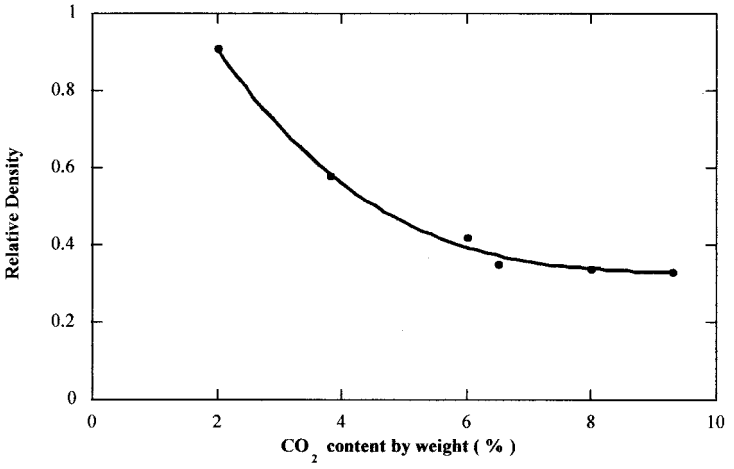

Figure 5 Relative densities as a function of CO_2 content. Foaming temperature was 175°C and foaming time was 30 s.

where $V_f = 1 - \rho_f/\rho$ is the void fraction; n, the number of cells in the SEM micrographs; M, the magnification of the micrograph; and A, the area of the micrograph (cm^2).

Tests of mechanical properties

Rectangular strip samples with dimensions of 50 × 10 mm^2 were used for the tensile tests. The thicknesses varied with the foam density and ranged from 1.5 to 4.2 mm. The tests were carried out at room temperature using an Instron testing machine with a 1000-lb-load cell at a constant crosshead rate of 1.0 mm/min. For each density, at least five samples were tested and the average data are reported in this article. The strain was calculated from the displacement of the crosshead, and the tensile modulus was determined by running a least-squares fit through the initial linear portions of the stress–strain curves.

RESULTS AND DISCUSSION

Sorption of CO_2 into polymer matrices

Figure 1 shows plots of CO_2 sorption in milligrams CO_2 per gram of polymer as a function of the saturation time at an 830-psi CO_2 saturation pressure and at room temperature. One can see that the CO_2 uptake in the polymer matrices increases quickly in the early stage of the sorption. After 60 h, the sorption reaches equilibrium for PSF, PPSF, and PESF, with the CO_2 concentration at equilibrium being 10% by weight for PSF, and 9 and 8%, for PPSF and PESF, respectively. For PEI and PEKK, however, the sorption did not attain equilibrium even after 120 h, and the CO_2 content at 120 h was 9 and 2.4% for these two polymers, respectively. Nonetheless, this gas concentration is sufficiently high for the microcellular foaming process. At such high gas concentrations, the roles of the solvent and the solute in the gas/polymer solution can be reversed,[4] where the gas serves as the solvent, and the polymer, as the solute. This reversal is crucial in the microcellular foaming process.

Electron micrographs

Some typical SEM micrographs of the foamed polymers are shown in Figure 2. The well-defined, very uniform foam structures obtained indicate that high-performance microcellular foams were successfully prepared. From the SEM micrographs, one can see that the resulting foams are closed-cell foams and the cell size is less than 10 μm, except for the PEKK foam. Under the same foaming conditions, the cell sizes of the PPSF and PEI foams (around 1 μm) were much smaller. PEKK is a semicrystalline polymer and it is very difficult for CO_2 to diffuse uniformly into this polymer matrix even after a very long period of time (120 h). The CO_2

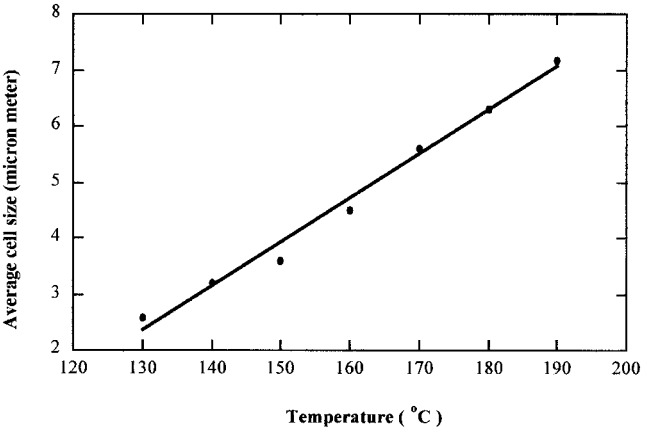

Figure 6 Average cell sizes as a function of foaming temperature. Foaming temperature was 175°C and foaming time was 30 s.

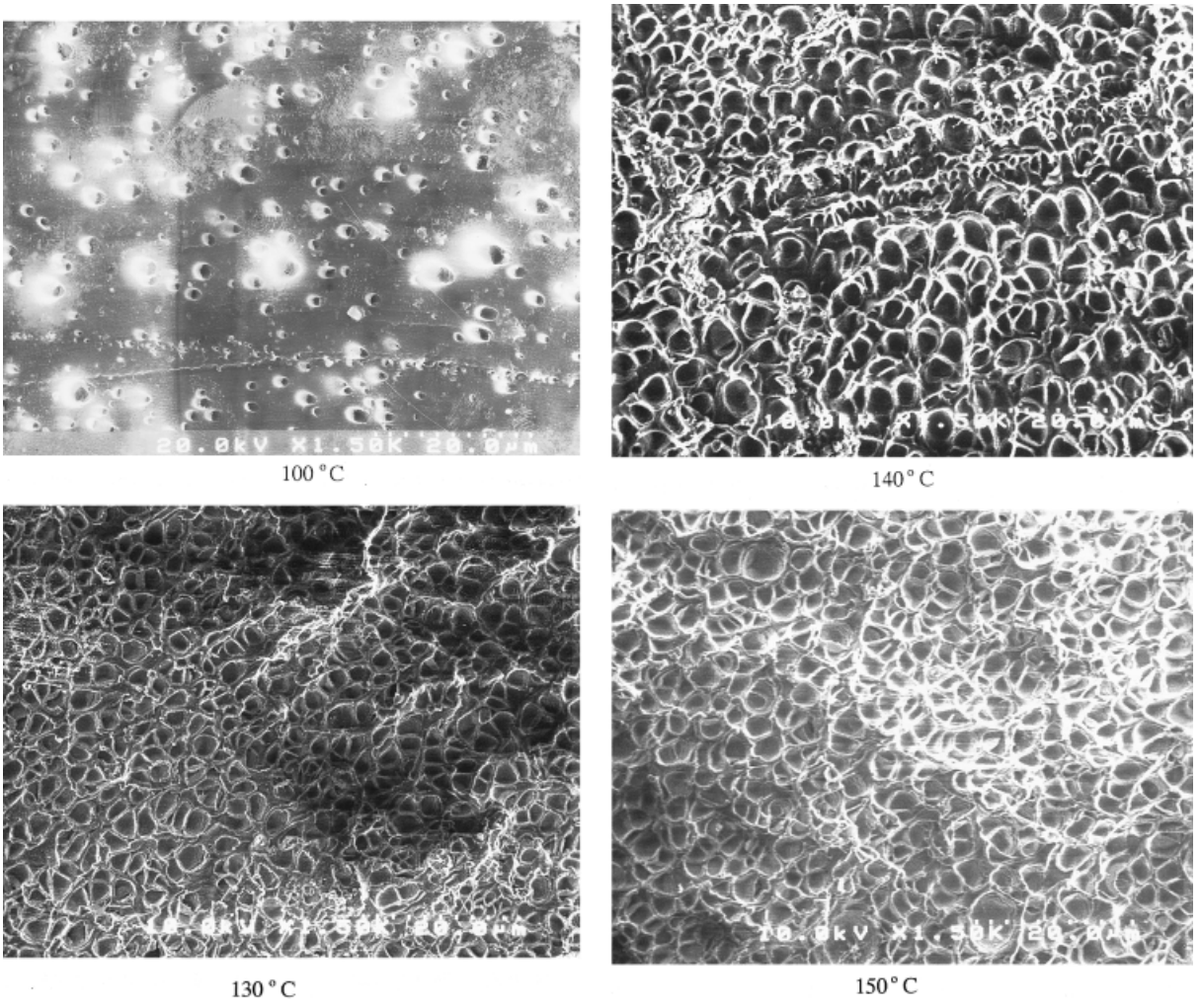

Figure 7 Some SEM micrographs for various foaming temperatures.

content in PEKK was only 2.4% and had a gradient which decreased from the edge to the center, causing the cell sizes to have a very broad distribution gradient inwardly. We also attempted to use thick samples, such as PSF and PEI rods of 10-mm diameters, but even after extremely long times (14 days), CO_2 still did not diffuse uniformly into the bulk sections of these samples. The SEM results showed that the middle portions were not foamed, as was the case for PEKK. A technique of the rapid solution formation needs to be developed for wider applications of this foaming technology.

Effects of foaming temperature on foam density

Figure 3 shows a plot of the relative density of the PSF foam as a function of the foaming temperature. In this experiment, the CO_2 content was about 9% by weight and the foaming time was 30 s. Relevant here is the fact that polymers can be plasticized by the dissolved gas.[22] Because of the high CO_2 concentration in the PSF matrix, the glass transition temperature, T_g, of the CO_2-saturated polymer was significantly lower than that of the pure polymer. This suggests that the cells can be nucleated at a temperatures well below the T_g of the pure polymer. In our experiment, we found that, for PSF, the lowest temperature at which significant cells were nucleated was 100°C, which is almost 90°C lower than the T_g of pure PSF. Figure 3 also shows that, with increase of the foaming temperature, the relative density of the PSF foams decreased to a minimum of about 0.28 at approximately 185°C and then began to increase quickly at higher temperature. This result is consistent with the increase in the average cell size and the slight decrease in cell density. When the temperature was increased further, the mobility of the polymer chains increased and the viscosity and the chain stiffness decreased, so the CO_2 molecules diffused out of the polymer matrix instead of supporting the desired cell nucleation and growth. As a result, the cells coalesced and the foam structures collapsed. Correspondingly, the foam density increased, as shown.

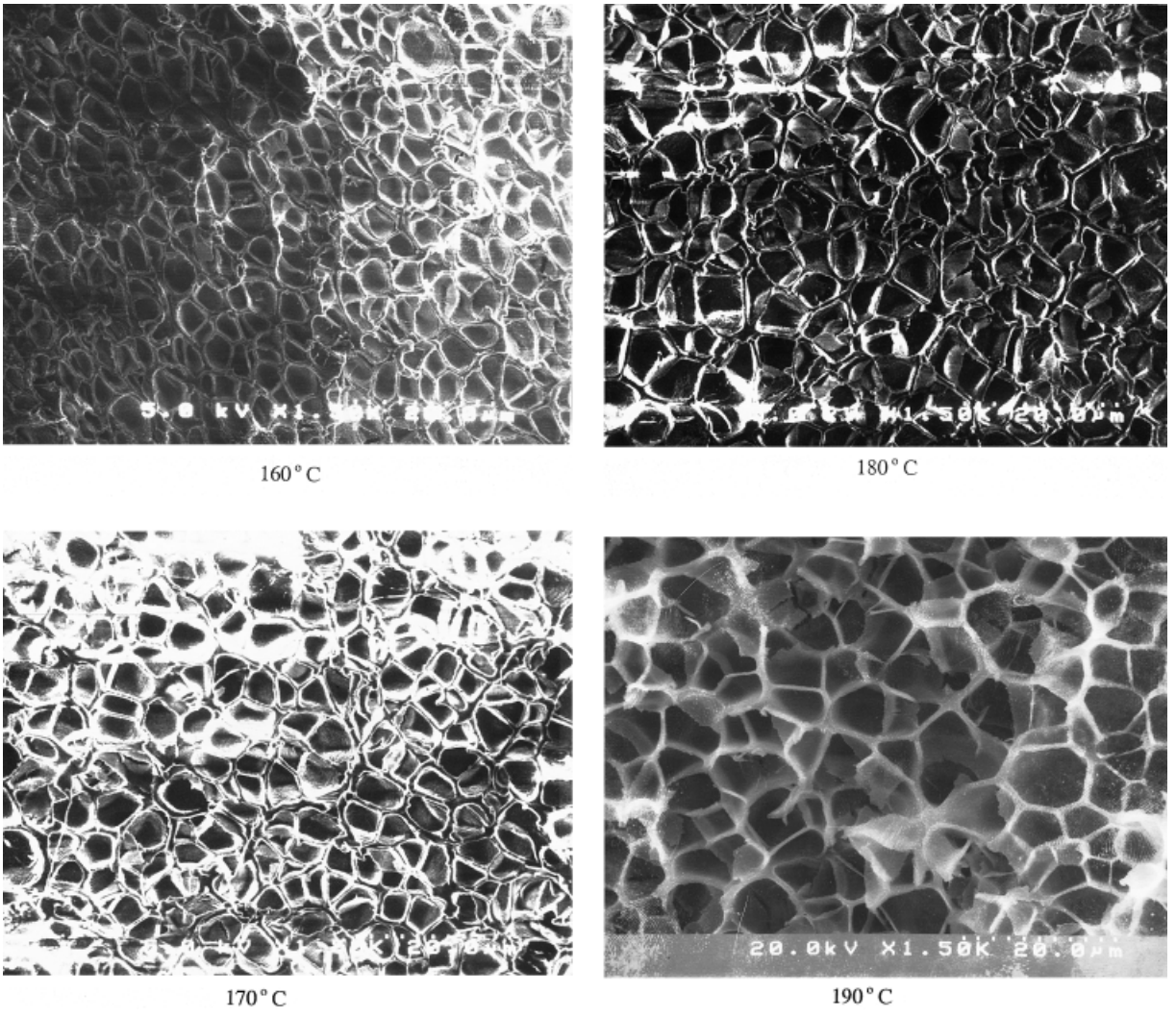

Figure 7 (*Continued from previous page*)

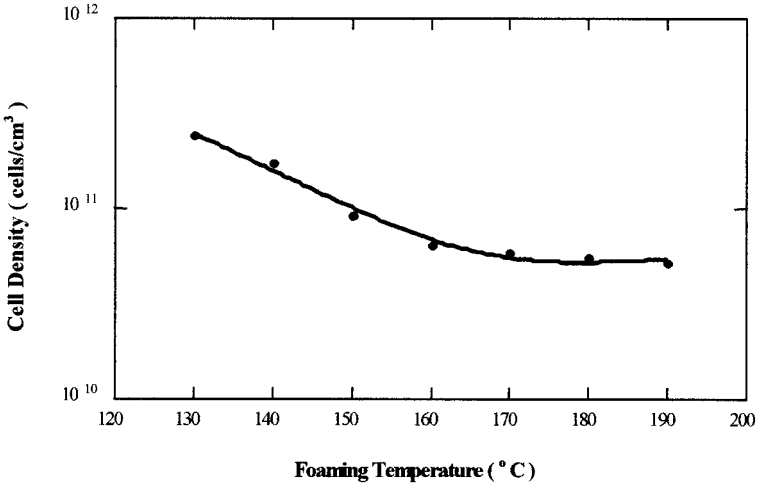

Figure 8 Cell densities as a function of foaming temperature.

TABLE I
Effects of Foaming Temperature on Densities, Cell Sizes, and Cell Densities

Foaming temperature (°C)	Relative density	Average cell size (μm)	10^{-10} Cell density (cells/cm^3)
130	0.72	2.6 (±0.49)	24.3
140	0.64	3.2 (±0.62)	17.2
150	0.52	3.6 (±0.52)	9.3
160	0.47	4.5 (±0.45)	6.4
170	0.40	5.6 (±0.63)	5.9
180	0.30	6.3 (±0.63)	5.6
190	0.26	7.2 (±0.56)	5.4

Effects of time on foam density

Results consistent with this analysis are presented in Figure 4. It shows the PSF foam relative density as a function of foaming time (at 9% CO_2). At low temperatures, the relative density decreased slightly as the foaming time increased, but when the foaming temperature was above 180°C, the foam density increased quickly with the foaming time, as shown by the results for 190 and 200°C in Figure 4.

Effect of co_2 content on the psf foam relative density

Figure 5 is a plot of PSF relative density as function of the CO_2 content. In this experiment, the foaming temperature was 175°C and the foaming time was 30 s. One can see that, with an increase in the CO_2 content in the polymer matrix, the relative density decreased. The more CO_2 molecules that diffuse into the polymer matrix, the more bubbles that are nucleated, and the lower the foam density. In our experiment, the SEM results show that when the CO_2 content is less than 4% by weight (which can be achieved by 16-h sorption) the middle portion of the polymer sheet could not be foamed. This means that the CO_2 could not diffuse into the bulk PSF sheet (1.5 mm in thickness) during a short period (about 16 h) to form a uniform gas/polymer solution. When the gas content was higher than 6.5% (24-h sorption), the relative density remained almost constant. This result implies that, for the PSF system, at least 24-h sorption time or 6.5% CO_2 is needed to obtain a uniform gas/polymer solution for the microcellular-foaming process.

Effect of foaming temperature on cell size and cell density

The average cell sizes of the PSF foams are plotted in Figure 6 as a function of the foaming temperature. In this experiment, the CO_2 was 9% by weight and the foaming time was 30 s for all the samples. One can see the average cell size increased linearly with the foaming temperature. When the foaming temperature was increased, the mobility of the polymer chains increased and the polymer viscosity decreased, and this permitted the cells to grow larger. Figure 7 presents SEM micrographs of the PSF foams in this experiment, arranged in the order of increasing foaming temperature. Figure 8 is a plot of cell density as a function of foaming temperature and shows that the cell nucleation density decreased slightly with an increase in the foaming temperature. These results are summarized in Table I. From these results and discussions, one can conclude that the structures of microcellular PSF foams (such as foam density, cell size, and cell density) can be controlled in the foaming process by careful choices of the foaming parameters (such as the gas content, foaming time, and foaming temperature).

Mechanical properties

Since these materials were prepared for possible use as structural materials, tensile tests were carried out on the PSF microcellular foams to investigate the de-

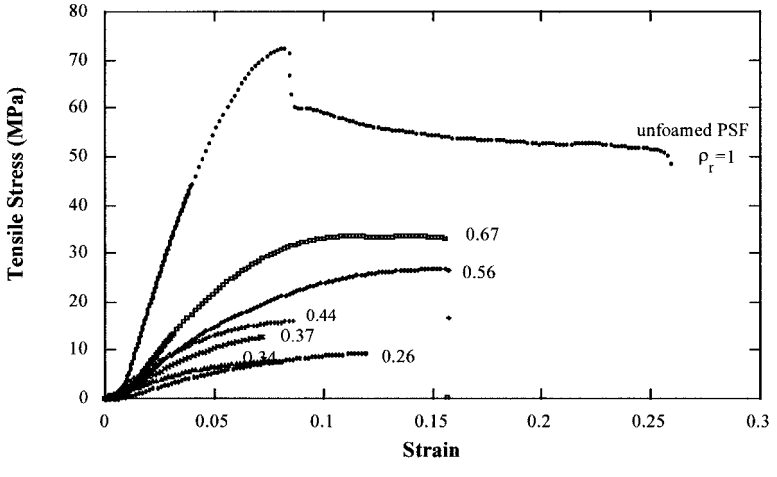

Figure 9 Tensile stress–strain curves of PSF microcellular foams.

TABLE II
Mechanical Properties of the Foams

Sample	Relative density	Tensile modulus (MPa)	Stress at break (MPa)	Strain at break (%)
Pure PSF	1	1390	64.1	26.7
T11	0.66	640	35.4	15.7
T16	0.62	470	27.0	14.6
T21	0.56	372	21.6	15.5
T26	0.44	339	16.1	8.7
T31	0.37	265	12.8	7.8
T36	0.34	173	8.36	8.2
T4	0.26	155	8.70	11.8

pendence of these properties on the foam relative densities. The stress–strain curves for microcellular polysulfone foams are shown in Figure 9, and Table II summarizes these experimental data. It should be noted that the specimens used in our tensile experiments had non-ASTM dimensions, and the thickness of the foam samples varied with the foam density, so there probably were some size effects in our tests.

Figure 9 and Table II show that, with a decrease in the relative density, the tensile strengths, the tensile moduli, and the elongation all decreased, as expected. Unfortunately, until now, there were only very limited data reported on the mechanical properties of such microcellular foams.[11,23,24]

According to the predictions of the current theory for conventional foams,[25] the tensile modulus of most closed-cell foams can be related to it density by the formula

$$E_f/E_m = (\rho_f/\rho_m)^2 \tag{2}$$

where E_f and E_m are the moduli of the foamed and unfoamed polymers, respectively, and ρ_f and ρ_m are the densities of the foamed and unfoamed polymers, respectively. The experimental results of the relative tensile modulus (E_f/E_m) are plotted together with the theoretically predicted values as a function of the relative density in Figure 10. The agreement between the experimental data and predicted values is excellent.

In the case of the tensile strength, the simple rule of mixtures gives the formula[11]

$$\sigma_f/\sigma_m = \rho_f/\rho_m \tag{3}$$

where σ_f and σ_m are the tensile stress at break of the foamed and unfoamed polymers, respectively. Figure 11 shows a comparison of the experimental tensile strengths and those predicted by the rule of mixtures. These experimental and theoretical results are also in very good agreement.

CONCLUSIONS

A series of commercially available high-temperature high-performance thermoplastics was successfully foamed in a two-stage batch microcellular foaming technology to give relatively homogeneous microcellular foams having cell sizes less than 10 μm, cell densities the order of 10^{10}–10^{14} cells/cm^3, and relative densities in the range 0.80–0.28. The structures of the microcellular foams were controlled by carefully choosing the foaming conditions, such as CO_2 content, foaming time, and foaming temperature. At least 24 h of sorption time were required to obtain a uniform gas/polymer solution in the CO_2/PSF system, in which the CO_2 is about 6.5% by weight. In the PSF foams, an increase in the foaming temperature gave increases in the average cell size, the cell density decreased slightly, and the relative density decreased to a minimum of about 0.28 at 185°C and then increased rapidly. The tensile moduli of these polysulfone foams increased with the square of their relative densities, and the tensile strengths were proportional to these

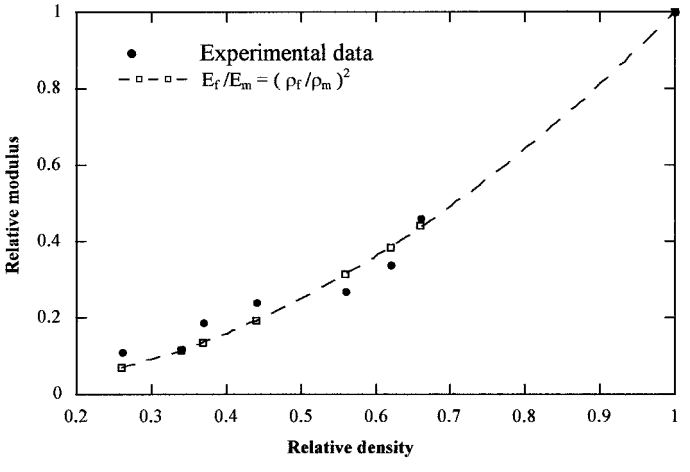

Figure 10 Relative tensile moduli as a function of relative foam density.

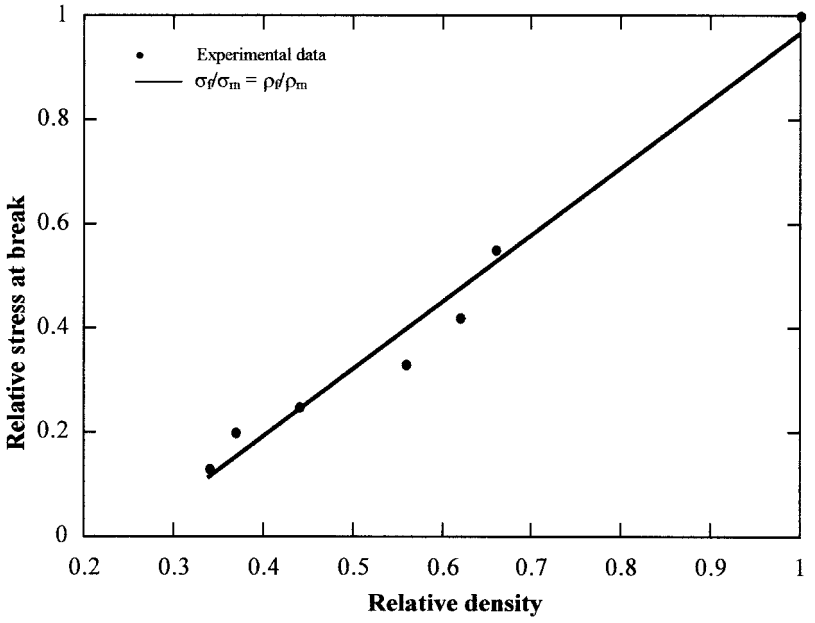

Figure 11 Relative tensile strengths as a function of relative foam density.

densities. Both of these experimental findings are in agreement with theory.

It is a pleasure for the authors to acknowledge the financial support provided by the Air Force Office of Scientific Research (Directorate of Chemistry and Materials Science) through Grant F49620-98-1-0319.

References

1. Martini, J. E.; Waldman, F. A.; Suh, N. P. U.S. Patent 4 473 665, 1984.
2. Martini, J. E.; Waldman, F. A.; Suh, N. P. SPE Tech Pap 28, 674, 1982.
3. Kumar V; Suh N. P. Polym Eng Sci 1990, 30, 1323.
4. Baldwin D. F.; Suh N. P. SPE ANTEC 1992, 1503.
5. Colton J. S.; Suh N. P. Polym Eng Sci 1987, 27, 485.
6. Arora, K. A.; Lesser, A. J.; McCarthy, T. J. Macromolecules 1998, 31, 4614.
7. Stafford, C. M.; Russell, T. P.; McCarthy, T. J. Macromolecules 1999, 32, 7610.
8. Park, C. B.; Cheung, L. K. Polym Eng Sci 1997, 37, 1.
9. Matuana, L. M.; Park, C. B.; Balatinecz, J. J Cell Polym 1998, 17, 1.
10. Kumar, V.; Weller, J. E.; Montecillo, R. SPE ANTEC 1992, 1452.
11. Kumar, V.; Van der Wel, M.; Weller, J. E.; Seeler, K. A. J Eng Mater Tech 1994, 116, 439.
12. Kumar, V.; Wing, G.; Pasricha, A.; Tuttle, M. SPE ANTEC 1993, 1832.
13. Kumar, V.; Weller, J. E. SPE ANTEC 1991, 1401.
14. Hirai, T.; Amano, N. SPE ANTEC 1993, 1256.
15. Kumar, V.; Gebizlioglu, O. S. SPE ANTEC 1991, 1297.
16. Baldwin, D. F.; Tate, D.; Park, C. B.; Cha, S. W.; Suh, N. P. J. Jpn Soc Polym Processing (SEIKEI-KAKOU) 1994, 6, 187.
17. Baldwin, D. F.; Tate, D.; Park, C. B.; Cha, S. W.; Suh, N. P. J Jpn Soc Polym Processing (SEIKEI-KAKOU) 1994, 6, 246.
18. Baldwin, D. F.; Gustafson, D. E.; Suh, N. P.; Shimbo, M. SPE ANTEC 1993, 1840.
19. Park, C. B.; Suh, N. P. Polym Eng Sci 1996, 36, 34.
20. Baldwin, D. F.; Park, C. B.; Suh, N. P. Polym Eng Sci 1996, 36, 1425.
21. Kumar, V.; Weller, J. E. SPE ANTEC 1991, 1401.
22. Goel, S. K.; Beckman, E. J. Polym Eng Sci 1994, 34, 1137.
23. Ozkul, M. H.; Mark, J. E.; Aubert, J. H. Mater Res Soc Symp Proc 1991, 207, 15
24. Ozkul, M. H.; Mark, J. E.; Aubert, J. H. J Appl Polym Sci 1993, 48, 767
25. Gibson, L. G.; Ashby, M. F. Cellular Solids: Structure and Properties; Pergamon: New York, 1988.